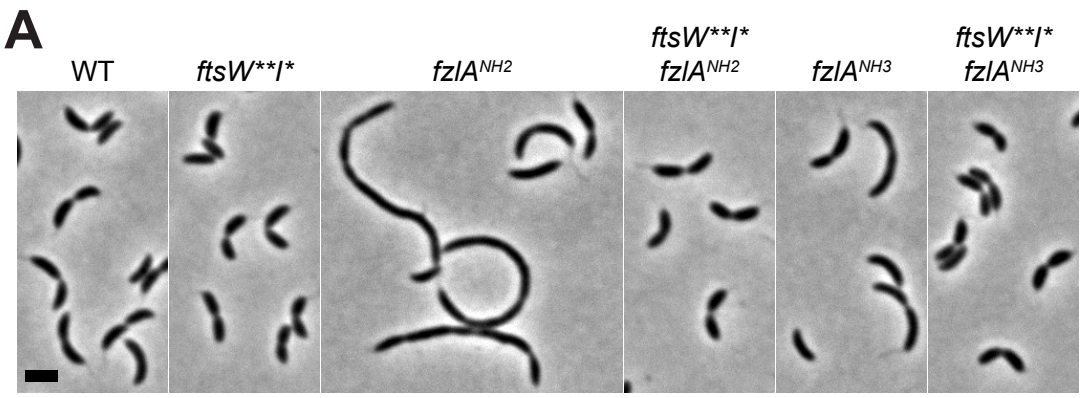
A
WT
ftsW**I*
fzlA^NH2
ftsW**I* fzlA^NH2
fzlA^NH3
ftsW**I* fzlA^NH3

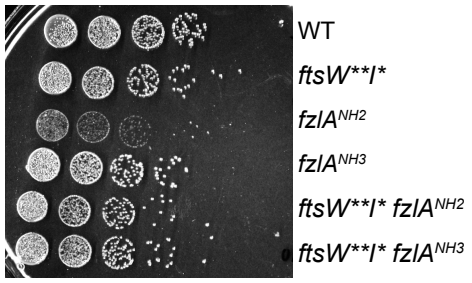
B
WT
ftsW**I*
fzlA^NH2
fzlA^NH3
ftsW**I* fzlA^NH2
ftsW**I* fzlA^NH3

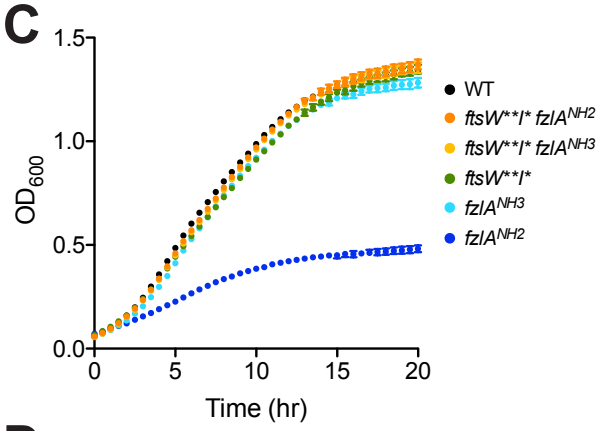
C
OD600
Time (hr)
WT
ftsW**I* fzlA^NH2
ftsW**I* fzlA^NH3
ftsW**I*
fzlA^NH3
fzlA^NH2

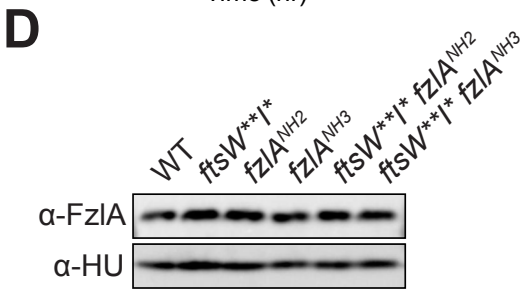
D
WT
ftsW**I*
fzlA^NH2
fzlA^NH3
ftsW**I* fzlA^NH2
ftsW**I* fzlA^NH3
α-FzlA
α-HU

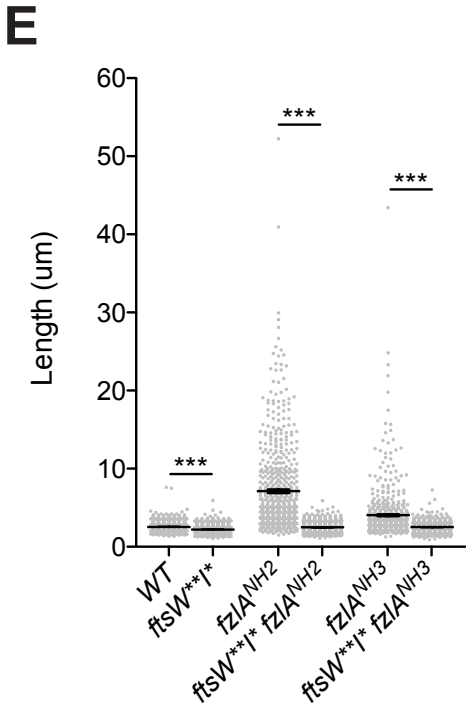
E
Length (um)
***
WT
ftsW**I*
fzlA^NH2
ftsW**I* fzlA^NH2
fzlA^NH3
ftsW**I* fzlA^NH3

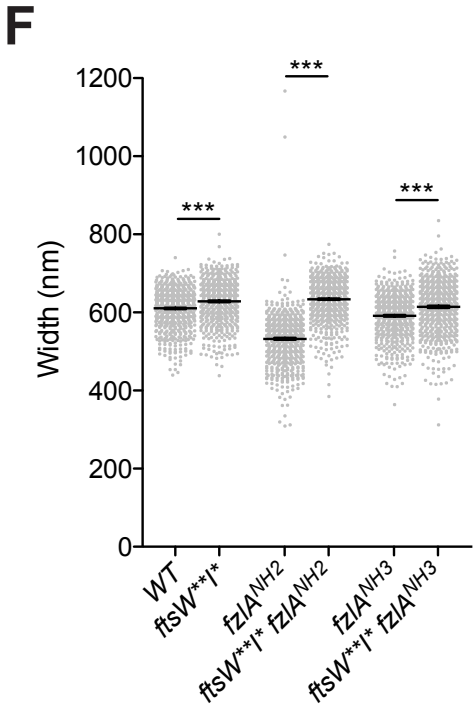
F
Width (nm)
***
WT
ftsW**I*
fzlA^NH2
ftsW**I* fzlA^NH2
fzlA^NH3
ftsW**I* fzlA^NH3

Figure S1. *ftsWI** rescue the fitness/morphological defects of two *fzlA* mutants. Related to Figure 1.**

(A) Phase contrast microscopy images depicting cells of the indicated strains. Scale bar = 2 μm. **(B, C)** Spot dilutions (diluted ten-fold) (B) and growth curves (C) of the indicated strains. **(D)** α-FzlA immunoblot (top) and α-HU immunoblot (bottom, loading control) of the indicated strains. **(E, F)** Lengths **(E)** and widths **(F)** of unsynchronized cells from the indicated strains. Mean ± SEM shown. Kruskal-Wallis tests with Dunn's post-test were performed to analyze differences compared to the indicated strains: $^{***}P \leq 0.001$. From left to right, n = 674, 609, 606, 653, 618, 645. Strain key (*Caulobacter crescentus*): WT (EG865), *ftsW**I* fzlA* (EG1557), $fzlA^{NH2}$ (EG1600), *ftsW**I** $fzlA^{NH2}$ (EG2111), $fzlA^{NH3}$ (EG1909), *ftsW**I** $fzlA^{NH3}$ (EG2489).

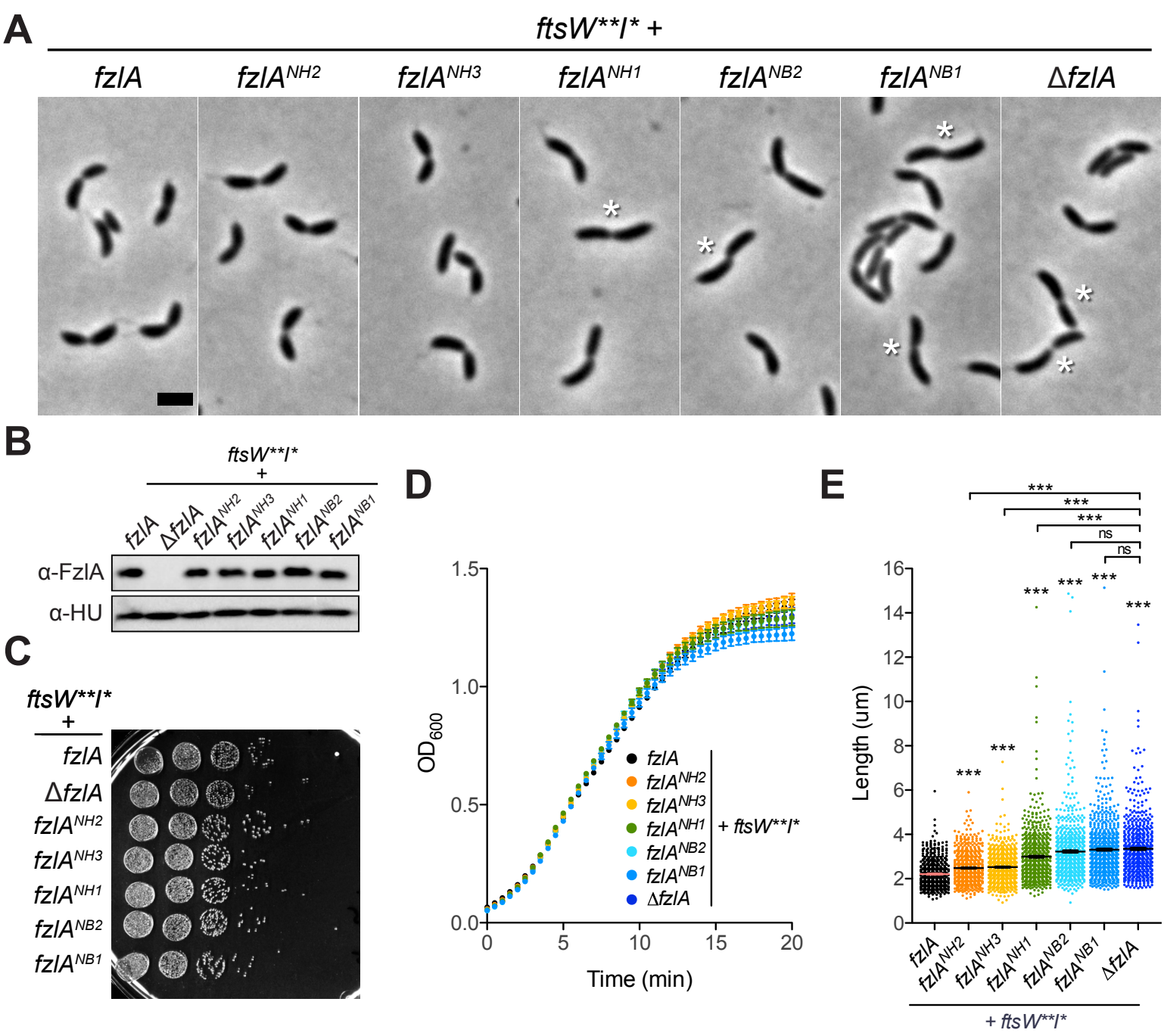
A
ftsW**I* +
fzlA
fzlA^NH2
fzlA^NH3
fzlA^NH1
fzlA^NB2
fzlA^NB1
ΔfzlA
B
ftsW**I*
+
fzlA
ΔfzlA
fzlA^NH2
fzlA^NH3
fzlA^NH1
fzlA^NB2
fzlA^NB1
α-FzlA
α-HU
C
ftsW**I*
+
fzlA
ΔfzlA
fzlA^NH2
fzlA^NH3
fzlA^NH1
fzlA^NB2
fzlA^NB1
D
OD600
Time (min)
+ ftsW**I*
E
Length (um)
ns
+ ftsW**I*

Figure S2. In the presence of hyperactive PG synthases, the interaction between FtsZ and FzlA determines division efficiency, but not growth rate or viability. Related to Figure 1.

(A) Phase contrast microscopy images depicting cells of the indicated strains. White asterisks mark S-shaped cells. Scale bar = 2 μm. **(B)** α-FzlA immunoblot (top) and α-HU immunoblot (bottom, loading control) of the indicated strains. **(C, D)** Spot dilutions (diluted ten-fold) **(C)** and growth curves **(D)** of the indicated strains. **(E)** Lengths of unsynchronized cells from the indicated strains. Mean ± SEM shown. Kruskal-Wallis tests with Dunn's post-test were performed to analyze differences compared to WT and the indicated strains: $^{ns}P>0.05$, $^{***}P\leq0.001$. From left to right, n = 609, 653, 645, 688, 674, 729, 612. Strain key (*Caulobacter crescentus*): *ftsW**I* fzlA* (EG1557), *ftsW**I* fzlA*^{NH2} (EG2111), *ftsW**I* fzlA*^{NH3} (EG2489), *ftsW**I* fzlA*^{NH1} (EG2492), *ftsW**I* fzlA*^{NB2} (EG2485), *ftsW**I* fzlA*^{NB1} (EG2495), *ftsW**I** Δ*fzlA* (EG2170).

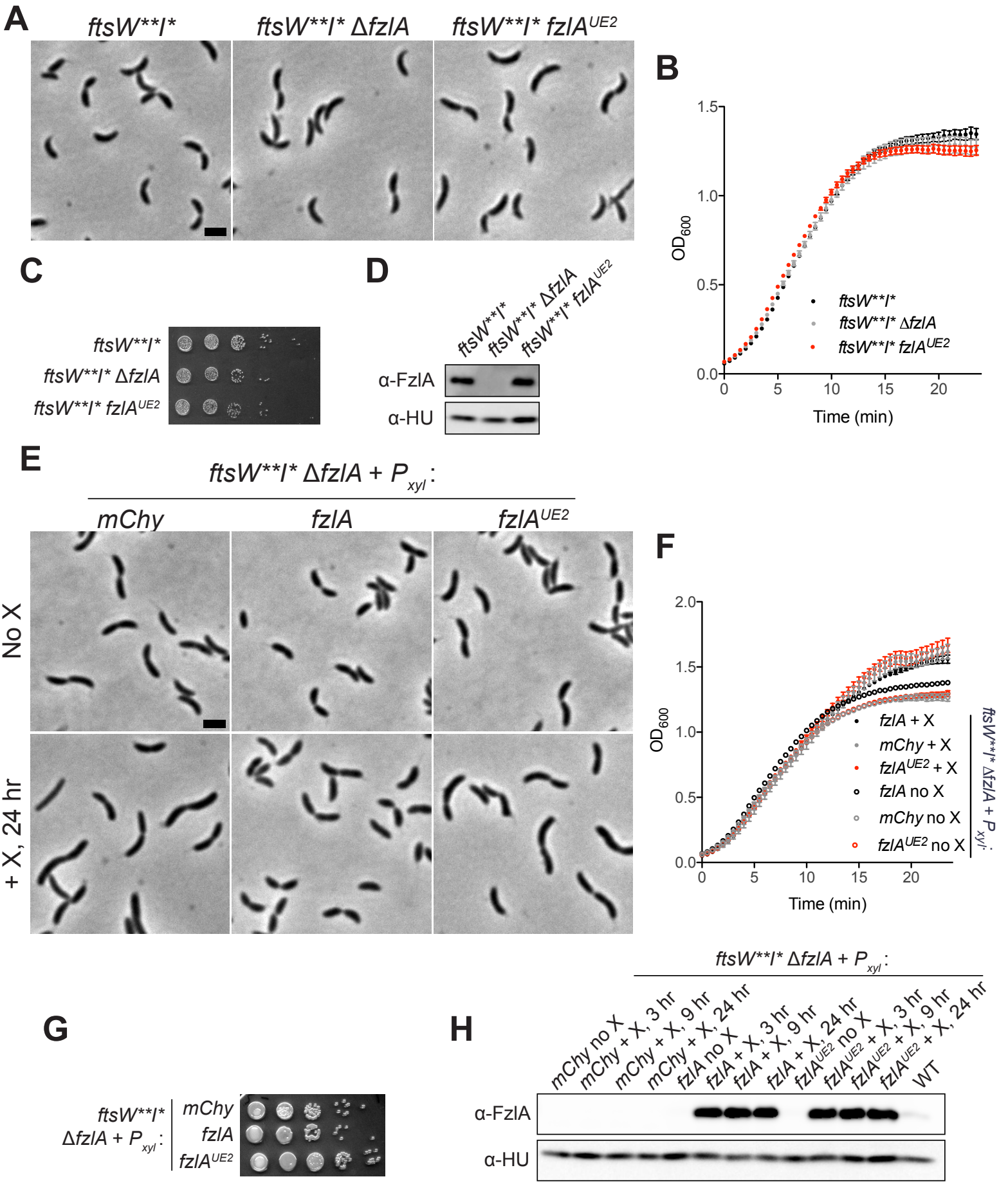
A
ftsW**I*
ftsW**I* ΔfzlA
ftsW**I* fzlA^UE2
B
OD600
Time (min)
ftsW**I*
ftsW**I* ΔfzlA
ftsW**I* fzlA^UE2
C
ftsW**I*
ftsW**I* ΔfzlA
ftsW**I* fzlA^UE2
D
α-FzlA
α-HU
E
ftsW**I* ΔfzlA + P xyl :
mChy
fzlA
fzlA^UE2
No X
+ X, 24 hr
F
OD600
Time (min)
fzlA + X
mChy + X
fzlA^UE2 + X
fzlA no X
mChy no X
fzlA^UE2 no X
ftsW**I* ΔfzlA + P xyl :
G
ftsW**I* ΔfzlA + P xyl :
mChy
fzlA
fzlA^UE2
H
ftsW**I* ΔfzlA + P xyl :
mChy no X
mChy + X, 3 hr
mChy + X, 9 hr
mChy + X, 24 hr
fzlA no X
fzlA + X, 3 hr
fzlA + X, 9 hr
fzlA + X, 24 hr
fzlA^UE2 no X
fzlA^UE2 + X, 3 hr
fzlA^UE2 + X, 9 hr
fzlA^UE2 + X, 24 hr
WT
α-FzlA
α-HU

Figure S3. Mutation of FzlA's essential C-terminus phenocopies loss of *fzlA* in an *ftsWI** background. Related to Figure 1.**

(A) Phase contrast microscopy images depicting cells of the indicated strains. Scale bar = 2 μm. **(B,C)** Growth curves **(B)** and spot dilutions (diluted ten-fold) **(C)** of the indicated strains. **(D)** α-FzlA immunoblot (top) and α-HU immunoblot (bottom, loading control) of the indicated strains. **(E)** Phase contrast microscopy images depicting cells of the indicated strains with no xylose (top) or incubated in the presence of 0.24% xylose (bottom) for 24 hours to control expression of the indicated gene. Scale bar = 2 μm. **(F)** Growth curves of the indicated strains with no xylose (no X) or incubated in the presence of 0.24% xylose (+X) to control expression of the indicated gene. **(G)** Spot dilutions (diluted ten-fold) of the indicated strains. **(H)** α-FzlA immunoblot (top) and α-HU immunoblot (bottom, loading control) of the indicated strains with no xylose (no X) or incubated in the presence of 0.24% xylose (+X) for 3, 9, or 24 hours to control expression of the indicated gene. Strain key (*Caulobacter crescentus*): *ftsW**I** (EG1557), *ftsW**I** Δ*fzlA* (EG2170), *ftsW**I** $fzlA^{UE2}$ (EG2895), *ftsW**I** Δ*fzlA* + P_{xyl} *mChy* (EG2879), *ftsW**I** Δ*fzlA* + P_{xyl} *fzlA* (EG2866), *ftsW**I** Δ*fzlA* + P_{xyl} $fzlA^{UE2}$ (EG2874).

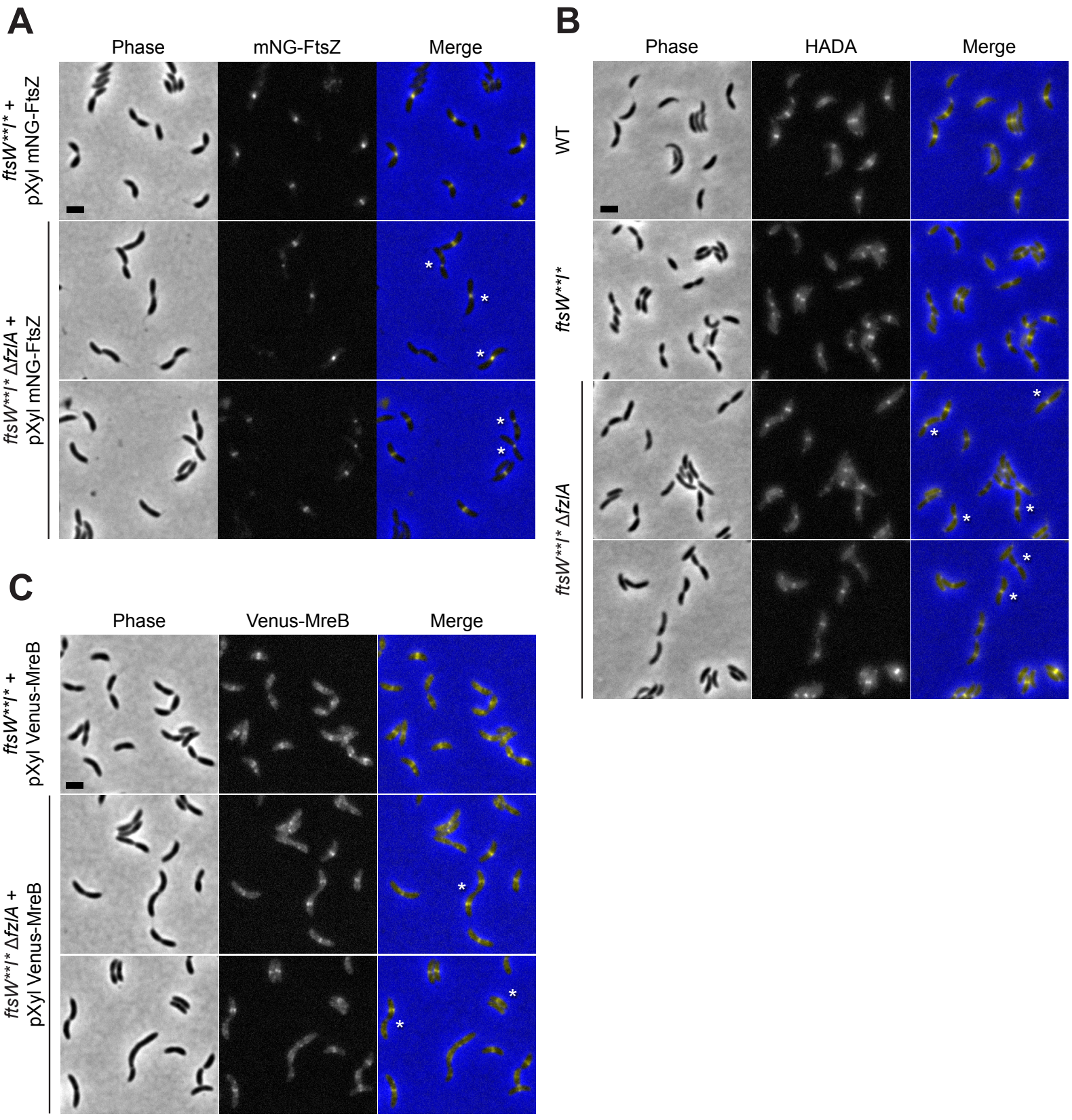
A
Phase
mNG-FtsZ
Merge
ftsW**I* + pXyl mNG-FtsZ
ftsW**I* ΔfzlA + pXyl mNG-FtsZ
B
Phase
HADA
Merge
WT
ftsW**I*
ftsW**I* ΔfzlA
C
Phase
Venus-MreB
Merge
ftsW**I* + pXyl Venus-MreB
ftsW**I* ΔfzlA + pXyl Venus-MreB

Figure S4. FtsZ, MreB, and PG synthesis localization is unaffected in *ftsWI** Δ*fzlA* cells. Related to Figure 3.**

(A) Phase contrast, fluorescence, and merged microscopy images depicting mNG-FtsZ localization in cells of the indicated strains in the presence of inducer (xylose). White asterisks mark S-shaped cells. Scale bar = 2 μm. **(B)** Phase contrast, fluorescence, and merged microscopy images depicting Venus-MreB localization in cells of the indicated strains in the presence of inducer (xylose). White asterisks mark S-shaped cells. Scale bar = 2 μm. **(C)** Phase contrast, fluorescence, and merged microscopy images depicting HADA localization in cells of the indicated strains after a 5 minute HADA pulse. White asterisks mark S-shaped cells. Scale bar = 2 μm. Strain key (*Caulobacter crescentus*): *ftsW**I* + pXyl mNG-ftsZ* (EG2157), *ftsW**I** Δ*fzlA + pXyl mNG-ftsZ* (EG2326), *ftsW**I* + pXyl Venus-mreB* (EG2377), *ftsW**I** Δ*fzlA + pXyl Venus-mreB* (EG2378), WT (EG865), *ftsW**I** (EG1557), *ftsW**I** Δ*fzlA* (EG2170).

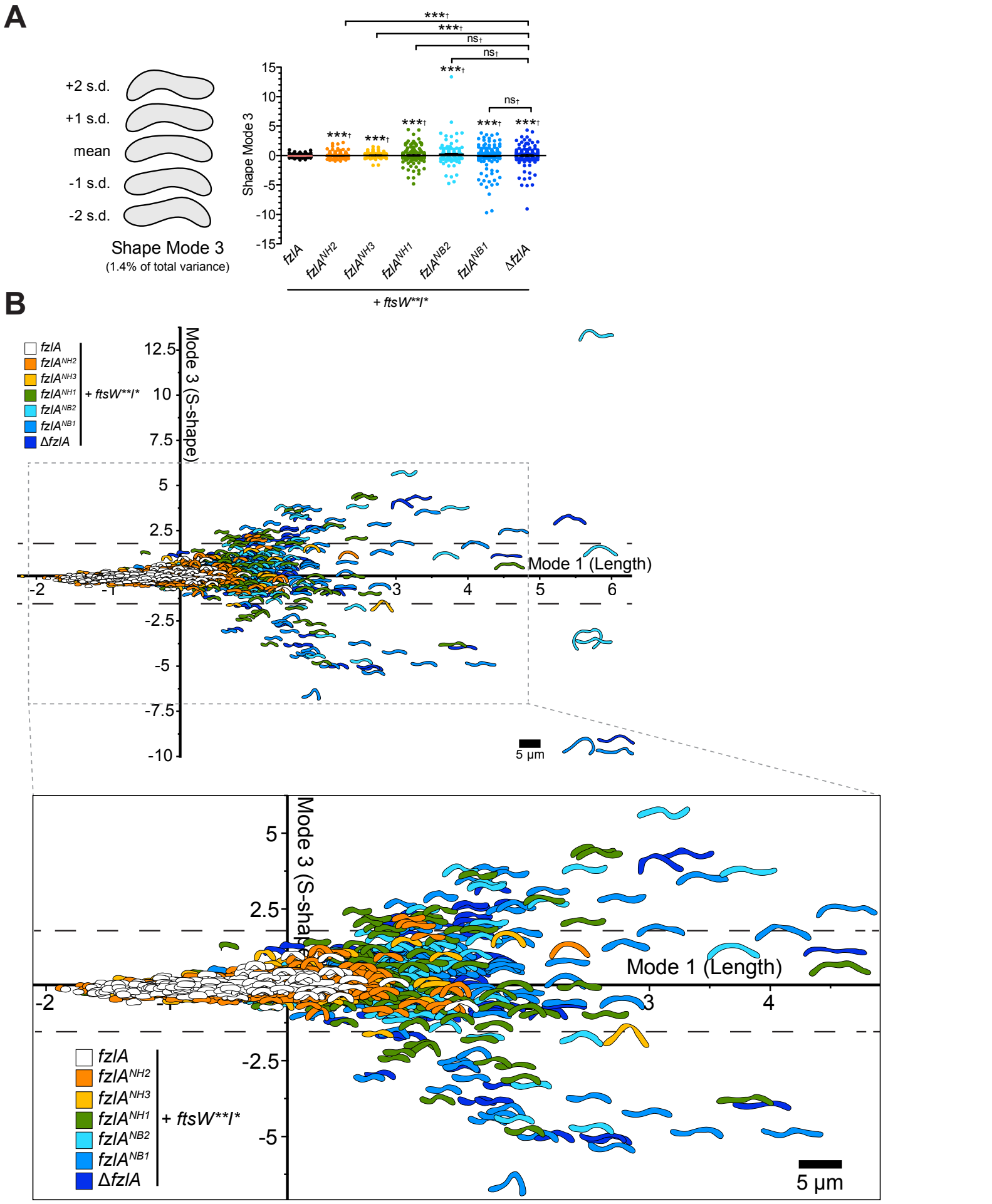
A
+2 s.d.
+1 s.d.
mean
-1 s.d.
-2 s.d.
Shape Mode 3
(1.4% of total variance)
Shape Mode 3
***†
***†
ns†
ns†
***†
ns†
***†
***†
***†
***†
***†
fzlA
fzlA^NH2
fzlA^NH3
fzlA^NH1
fzlA^NB2
fzlA^NB1
ΔfzlA
+ ftsW**I*
B
fzlA
fzlA^NH2
fzlA^NH3
fzlA^NH1
fzlA^NB2
fzlA^NB1
ΔfzlA
+ ftsW**I*
Mode 3 (S-shape)
Mode 1 (Length)
5 µm
Mode 3 (S-shape)
Mode 1 (Length)
5 µm

Figure S5. Interaction of FtsZ with FzlA is necessary for proper division site shape maintenance. Related to Figure 3.

(A) PCA of cell shape in a population of unsynchronized cells (not all cells are necessarily actively constricting) from the indicated strains. Shape mode 3 approximately captures degree of S-shape in cells. Mean cell contour ± 1 or 2 standard deviations (s.d.) is shown (left). Shape mode values for cells in each strain are plotted and mean ± SEM is shown (right). A Brown-Forsythe Levene-type test (which is used in populations not assumed to be normally distributed) was performed to determine differences between population variances (†): $^{ns}P>0.05$, $^{***}P\leq0.001$. From left to right, n = 269, 375, 218, 250, 177, 289, 211. **(B)** Plot of shape mode 3 (degree of S-shape) vs. shape mode 1 (length) values in a population of unsynchronized cells (not all cells are necessarily actively constricting) from the indicated strains. The dashed lines qualitatively demark the boundary between cells that appear to be S-shaped and those that display normal curvature. Inset presents a zoomed in view of the highlighted region of interest. Strain key (*Caulobacter crescentus*): *ftsW**I* fzlA* (EG1557), *ftsW**I* fzlA*^{NH2} (EG2111), *ftsW**I* fzlA*^{NH3} (EG2489), *ftsW**I* fzlA*^{NH1} (EG2492), *ftsW**I* fzlA*^{NB2} (EG2485), *ftsW**I* fzlA*^{NB1} (EG2495), *ftsW**I** Δ*fzlA* (EG2170).

A

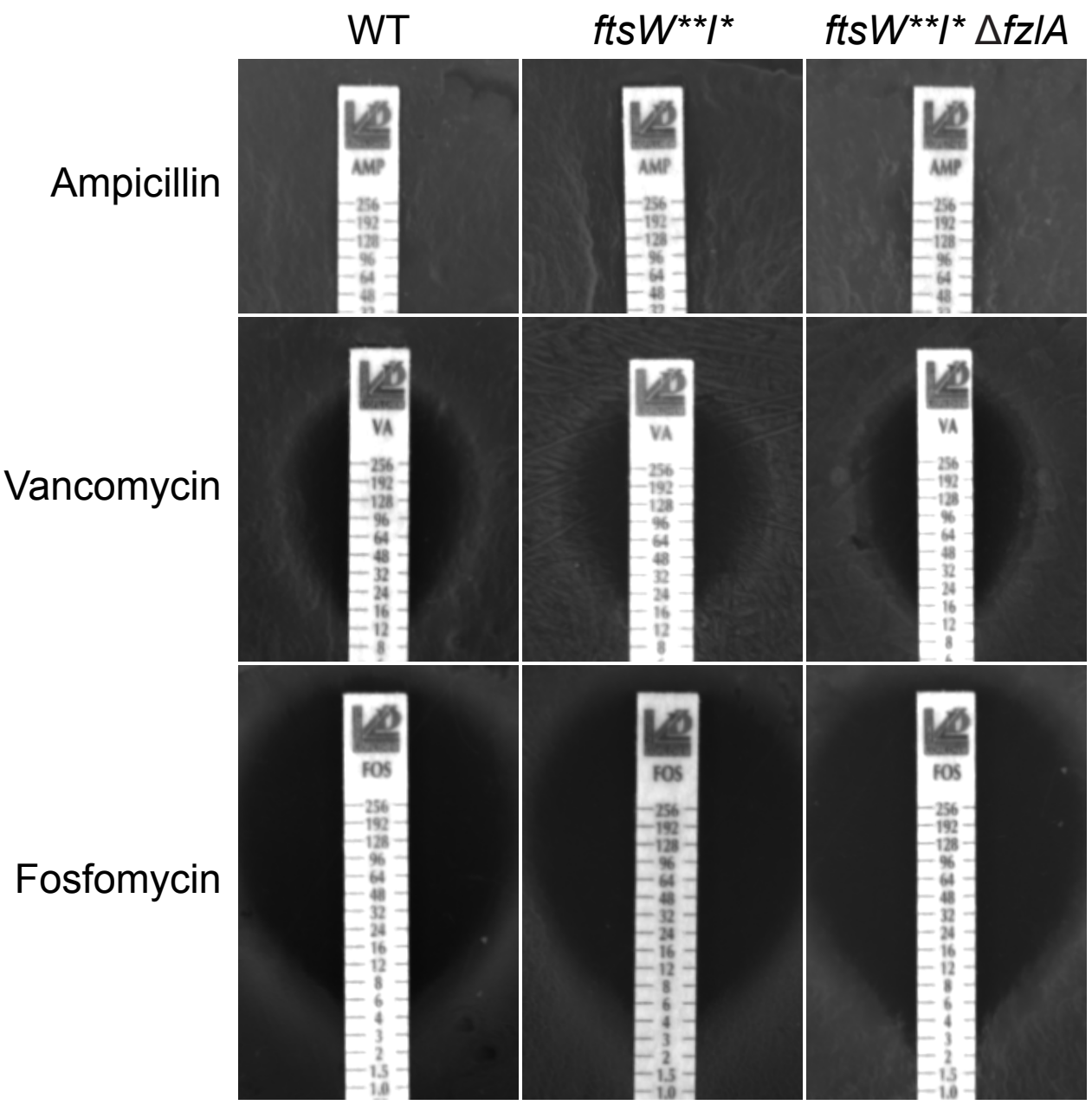
WT
ftsW**I*
ftsW**I* ΔfzlA
Ampicillin
Vancomycin
Fosfomycin
AMP
VA
FOS
256
192
128
96
64
48
32
24
16
12
8
6
4
3
2
1.5
1.0

B

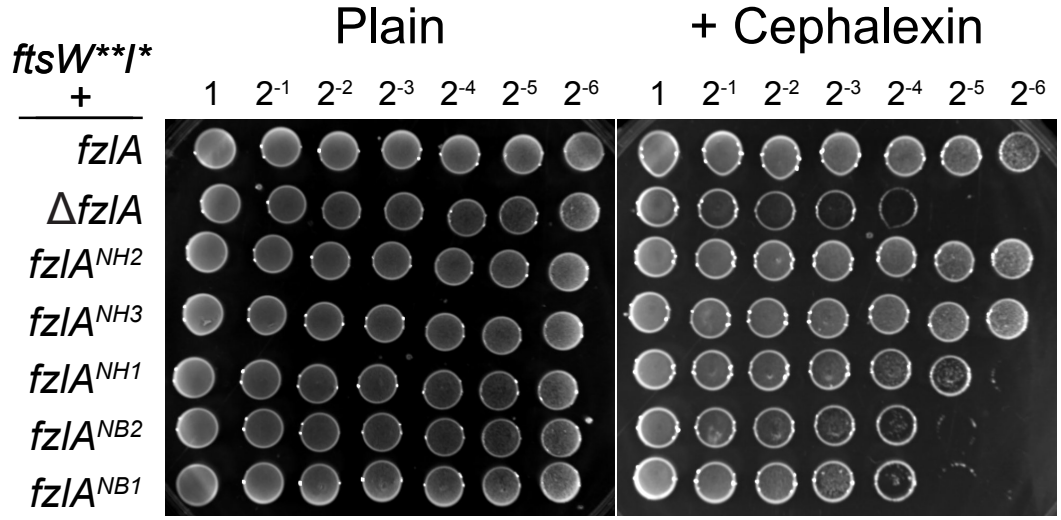
ftsW**I*
+
Plain
+ Cephalexin
1
2-1
2-2
2-3
2-4
2-5
2-6
fzlA
ΔfzlA
fzlANH2
fzlANH3
fzlANH1
fzlANB2
fzlANB1

Figure S6. Effect of loss of FzlA and FzlA-FtsZ interaction on resistance to cell wall antibiotics. Related to Figure 4.

(A) Plates of the indicated strains grown in the presence of antibiotic minimum inhibitory concentration (MIC) test strips, with antibiotic concentration decreasing from top to bottom. **(B)** Spot dilutions (diluted two-fold) of the indicated strains plated on PYE ± cephalexin (6 μg/ml). Strain key (*Caulobacter crescentus*): WT (EG865), *ftsW**I* fzlA* (EG1557), *ftsW**I* fzlA*^{NH2} (EG2111), *ftsW**I* fzlA*^{NH3} (EG2489), *ftsW**I* fzlA*^{NH1} (EG2492), *ftsW**I* fzlA*^{NB2} (EG2485), *ftsW**I* fzlA*^{NB1} (EG2495), *ftsW**I** Δ*fzlA* (EG2170), *fzlA*^{NH2} (EG1600), *fzlA*^{NH3} (EG1909).

Supplemental References

S1. Thanbichler, M., Iniesta, A.A., and Shapiro, L. (2007). A comprehensive set of plasmids for vanillate- and xylose-inducible gene expression in Caulobacter crescentus. Nucleic Acids Res. *35*, e137.

S2. Goley, E.D., Comolli, L.R., Fero, K.E., Downing, K.H., and Shapiro, L. (2010). DipM links peptidoglycan remodelling to outer membrane organization in Caulobacter. Mol. Microbiol. *77*, 56–73.

S3. Goley, E.D., Dye, N.A., Werner, J.N., Gitai, Z., and Shapiro, L. (2010). Imaging-based identification of a critical regulator of FtsZ protofilament curvature in Caulobacter. Mol. Cell *39*, 975–987.

S4. Lariviere, P.J., Szwedziak, P., Mahone, C.R., Löwe, J., and Goley, E.D. (2018). FzlA, an essential regulator of FtsZ filament curvature, controls constriction rate during Caulobacter division. Mol. Microbiol. *107*, 180–197.

S5. Goley, E.D., Yeh, Y.-C., Hong, S.-H., Fero, M.J., Abeliuk, E., McAdams, H.H., and Shapiro, L. (2011). Assembly of the Caulobacter cell division machine. Mol. Microbiol. *80*, 1680–1698.

S6. Meier, E.L., Daitch, A.K., Yao, Q., Bhargava, A., Jensen, G.J., and Goley, E.D. (2017). FtsEX-mediated regulation of the final stages of cell division reveals morphogenetic plasticity in Caulobacter crescentus. PLOS Genet. *13*, e1006999.

S7. Thanbichler, M., and Shapiro, L. (2006). MipZ, a Spatial Regulator Coordinating Chromosome Segregation with Cell Division in Caulobacter. Cell *126*, 147–162.

S8. Figueroa-Cuilan, W., Daniel, J.J., Howell, M., Sulaiman, A., and Brown, P.J.B. (2016). Mini-Tn7 Insertion in an Artificial attTn7 Site Enables Depletion of the Essential Master Regulator CtrA in the Phytopathogen Agrobacterium tumefaciens. Appl. Environ. Microbiol. *82*, 5015–5025.

S9. Choi, K.-H., Mima, T., Casart, Y., Rholl, D., Kumar, A., Beacham, I.R., and Schweizer, H.P. (2008). Genetic tools for select-agent-compliant manipulation of Burkholderia pseudomallei. Appl. Environ. Microbiol. *74*, 1064–1075.

S10. Howell, M., Aliashkevich, A., Sundararajan, K., Daniel, J.J., Lariviere, P.J., Goley, E.D., Cava, F., and Brown, P.J.B. (2019). Agrobacterium tumefaciens divisome proteins regulate the transition from polar growth to cell division. Mol. Microbiol. Available at: https://onlinelibrary.wiley.com/doi/abs/10.1111/mmi.14212 [Accessed January 31, 2019].

S11. Watson, B., Currier, T.C., Gordon, M.P., Chilton, M.D., and Nester, E.W. (1975). Plasmid required for virulence of Agrobacterium tumefaciens. J. Bacteriol. *123*, 255–264.

S12. Evinger, M., and Agabian, N. (1977). Envelope-associated nucleoid from Caulobacter crescentus stalked and swarmer cells. J. Bacteriol. *132*, 294–301.

S13. Modell, J.W., Kambara, T.K., Perchuk, B.S., and Laub, M.T. (2014). A DNA Damage-Induced, SOS-Independent Checkpoint Regulates Cell Division in Caulobacter crescentus. PLOS Biol *12*, e1001977.